Journal of Hazardous Materials 178 (2010) 553–559

Contents lists available at ScienceDirect

Journal of Hazardous Materials

journal homepage: www.elsevier.com/locate/jhazmat

Kinetics and mechanism studies of *p*-nitroaniline adsorption on activated carbon fibers prepared from cotton stalk by $NH_4H_2PO_4$ activation and subsequent gasification with steam

Kunquan Li[a,b], Ye Li[b], Zheng Zheng[a,*]

[a] Environmental Science & Engineering Department, Fudan University, Shanghai 200433, China
[b] College of Engineering, Nanjing Agricultural University, Nanjing 210031, China

ARTICLE INFO

Article history:
Received 18 September 2009
Received in revised form 24 January 2010
Accepted 25 January 2010
Available online 1 February 2010

Keywords:
Activated carbon fiber
Cotton stalk
p-Nitroaniline
Kinetics

ABSTRACT

Activated carbon fibers (ACFs) were prepared for the removal of *p*-nitroaniline (PNA) from cotton stalk by chemical activation with $NH_4H_2PO_4$ and subsequent physical activation with steam. Surface properties of the prepared ACFs were performed using nitrogen adsorption, FTIR spectroscopy and SEM. The influence of contact time, solution temperature and surface property on PNA adsorption onto the prepared ACFs was investigated by conducting a series of batch adsorption experiments. The kinetic rates at different temperatures were modeled by using the Lagergren-first-order, pseudo-second-order, Morris's intraparticle diffusion and Boyd's film-diffusion models, respectively. It was found that the maximum adsorption of PNA on the ACFs was more than 510 mg/L, and over 60% adsorption occurred in first 25 min. The effect of temperature on the adsorption was related to the contacting time and the micropore structure of the adsorbents. And the increase of micropore surface area favored the adsorption process. Kinetic rates fitted the pseudo-second-order model very well. The pore diffusion played an important role in the entire adsorption period, and intraparticle diffusion was the rate-limiting step in the beginning 20 min. The Freundlich model provided a better data fitting as compared with the Langmuir model. The surface micrograph of the ACF after adsorption showed a distinct roughness with oval patterns. The results revealed that the adsorption was in part with multimolecular layers of coverage.

1. Introduction

p-Nitroaniline (PNA) can be found in wastewater discharges from industries where it is either manufactured or used as an intermediate such as azo dyes, antioxidants, fuel additives, pesticides, antiseptic agents and medicines for poultry [1]. PNA is highly toxic with a TLV (Threshold Limit Value) of 0.001 kg/m^3. The presence of PNA in water may cause long-term adverse effects in the aquatic environment in terms of its hematoxicity, splenotoxicity and nephrotoxicity [2–4]. Therefore it has been enlisted as one of the major contaminants in water worldwide.

Various attempts have been made for PNA removal from aqueous solutions, which include hydrothermal decomposition [5], Fenton oxidation [6], photocatalytic degradation [7], biodegradation [8], adsorption [9–11] and others [12–13]. Adsorption has been shown to be one most promising technology for PNA removal. Activated carbon fibers (ACFs) are novel and fibrous carbonaceous adsorbents. ACFs have many favorable characteristics such as high adsorption capacity and high mass transfer rate for both adsorption or desorption, and are easy to be handled in a batch adsorber as compared with granular and powdered AC [14,15]. Therefore, ACFs have received increasing attention in recent years as adsorbents for water treatment [16,17]. However, the kinetic and mechanism of PNA adsorption onto ACF was seldom reported [18].

As cotton is one major crop in China, which cultivation area surpass 5.5 million hectare, and as much as 20 million tons (dry weight) of cotton stalk are produced annually [19], a better way for the exploitation of this cheap and abundant agricultural by-products is to turn it into ACFs. In our previous work, ACFs have successfully prepared from cotton stalk fiber for PNA removal by activation with KH_2PO_4 and gasification with steam [18]. In this paper, we will explain the adsorption of PNA on the ACFs prepared from cotton stalk fiber by chemical activation with $NH_4H_2PO_4$ and subsequent physical activation with steam.

The aim of this work is to evaluate the adsorption potential of the ACFs prepared from cotton stalk fiber for the removal of PNA from aqueous solution. Influencing factors on PNA adsorption, including contact time, temperature and surface property of the ACFs

* Corresponding author. Tel.: +86 21 65643342; fax: +86 25 58606540.
E-mail address: hjzzheng@fudan.edu.cn (Z. Zheng).

0304-3894/$ – see front matter.
doi:10.1016/j.jhazmat.2010.01.120

Nomenclature

B	constant in Eq. (9)
C_0	initial concentration of adsorbate in solution (mg/L)
C_e	concentration of adsorbate in solution at equilibrium (mg/L)
C_t	concentration of adsorbate in solution at any time t (mg/L)
c_w	resistance to mass transfer in the external liquid film (mg/g)
D_i	effective diffusivity of solute within the particle (cm^2/s)
F	fractional attainment of equilibrium at time t
$h_{0,1}$	initial rate of adsorption of Lagergren-first-order model (mg/(g min))
$h_{0,2}$	initial rate of adsorption of pseudo-second-order model (mg/(g min))
k_1	rate constant of Lagergren-first-order kinetic model (min^{-1})
k_2	rate constant of Ho's pseudo-second-order kinetic model (g/(mg min))
K_L	Langmuir constant related to the energy of adsorption (L/mg)
K_F	adsorption capacity parameter of Freundlich ($(mg/L)^{1/n}$)
K_w	intraparticular diffusion rate ($mg/(g\,min^{0.5})$)
n_b	integer that defines the infinite series solution
n_F	isotherm exponent of Freundlich equation
N	number of measurements made
q^0	maximum mass of adsorbate adsorbed on the adsorbent (mg/g)
q_e	amount of adsorbate adsorbed on the adsorbent at equilibrium (mg/g)
q_t	amount of adsorbate adsorbed on the adsorbent at any time t (mg/g)
$q_{t,exp}$	experimental amount of adsorbate adsorbed on the adsorbent (mg/g)
$q_{t,cal}$	calculated amount of adsorbate adsorbed on the adsorbent (mg/g)
r_p	particle radius of adsorbent particle, assumed to be spherical (cm)
t	time (min)
V	solution volume (L)
W	mass of adsorbent (g)

were investigated, and the adsorption mechanism was suggested according to the kinetic experimental results.

2. Experimental

2.1. Adsorbent

2.1.1. Preparation of ACFs

The precursor used for the production of ACFs was cotton stalk fiber provided by Hubei Chemical Fiber Co., China. A horizontal tubular furnace with an artificial intelligence temperature controller AI708P and a 60 cm tubular ceramic insert was used for the production of the carbon. Raw cotton stalk fiber was impregnated with a 4% $NH_4H_2PO_4$ solution with a mass ratio of 1:60 and stirred for 60 min. Then the mixed precursors were filtered and dried in an oven at 105 °C. After that, ten grams of the mixed precursors were placed in a 10 cm stainless steel container positioned in the horizontal tubular furnace. Stabilization was carried out by heating to 250 °C at a rate of 10 °C/min under a constant high purity nitrogen flow of 80 cm^3/min and by maintaining the temperature for 60 min. The carbonization was then carried out by raising the temperature at a rate of 10 °C/min to 600 °C, and maintaining the temperature for 30 min. The furnace was then heated (10 °C/min) to different target temperature and the gas flow was switched to a water steam. Different reaction times were then applied for the production of cotton stalk ACF. The ACF activated at 800 °C for 30 min is referred to as CS800, and the sample activated at 850 °C for 20 min is referred to as CS850. The resultant ACFs were cooled in a stream of gaseous nitrogen. In order to remove all the chemicals and mineral matters, the prepared ACFs were washed with HCl (0.1 mol/L) for at least 12 h, and then were rinsed with deionized water in a soxhlet extractor until the washing water pH was in the range of 6–7.

2.2. Surface properties

2.2.1. Measurement of pore structure

The pore structures of the ACFs were characterized by nitrogen adsorption at −196 °C by using a computer controlled automated porosimeter (Micromeritics ASAP-2020, America). Prior to adsorption, the sample was out-gassed under vacuum at 300 °C for 12 h. Nitrogen adsorption isotherms were analyzed by applying the standard Brunauer–Emmett–Teller (BET) equation to calculate the specific surface area (S_{BET}), and the t-plot method was used to calculate the micropore volume (V_{micro}). The total pore volume (V_{total}) was deduced from the adsorption data based on the manufacturer's software, and the pore size distribution was derived from the density functional theory (DFT). The t-plot method was used to calculate the micropore volume (V_{micro}) and the exterior surface area (S_{ext}). The micropore surface area (S_{micro}) was obtained from S_{BET} minus S_{ext}.

2.2.2. Scanning electron microscopy

A scanning electron microscope (Hitachi S4800, Japan) was used to visualize the surface morphology and structure of CS850 before and after adsorption of PNA.

2.2.3. Elemental analysis

The elemental analysis of the adsorbent was obtained from a CHN-O-Rapid elemental analytical instrument (Elementer, Germany).

2.2.4. Fourier transform infrared spectroscopy (FTIR)

The surface functional groups of the adsorbent were detected by FTIR (NEXUS870, America-Nicolet). The pH at the point of zero charge (pH_{pzc}) was determined by a batch equilibrium method described by Babic [20].

2.3. Chemicals

All the reagents used were of analytical grade and without further purification. The chemicals used in this study, i.e., $NH_4H_2PO_4$, HCl, NaOH and PNA, were purchased from Shanghai Chemical Reagent Co., China. PNA solution (200 mg/L) was prepared by dissolving required amount of PNA in distilled water in the adsorption test.

2.4. Adsorption studies

In batch adsorption experiments, different doses of adsorbent (0.10–1.30 g/L) were added into several 250 mL Erlenmeyer flasks, each containing 100 mL PNA solution (200 mg/L) at 25 °C in order to determine the adsorption isotherms and to evaluate the effect of temperature on PNA adsorption. Following this, the flasks were

shaken at 150 rpm at a pre-settled temperature for 24 h in a constant temperature shaker (Shanghai Scientific Instrument Co. Ltd., China). Samples were filtrated, and then the concentrations of PNA at equilibrium (C_e) were determined.

In kinetic studies, batch experiments were conducted at different periods by adding 0.2415 g adsorbent into each 500 mL PNA solution at 25, 35, 45 and 55 °C, respectively. Samples were collected periodically at every 5 min for the first 30 min and then at every 15 min for kinetic studies.

The amount of PNA adsorbed per unit mass of adsorbent at time t (q_t) and at equilibrium (q_e) was calculated according to the following two equations:

$$q_e = \frac{V(C_0 - C_e)}{W} \quad (1)$$

$$q_t = \frac{V(C_0 - C_t)}{W} \quad (2)$$

2.5. Analysis

The concentrations of PNA were analyzed by using a Helious Betra UV–vis spectrometer (Unicam Co., UK) that gave good linearity for the absorbency versus PNA concentration at its maximum absorbency wavelength 381 nm. In order to prevent pH from affecting absorbency of PNA samples, all samples were basified to a pH level of 8.0 by addition of 0.1 mol/L sodium hydroxide.

3. Results and discussion

3.1. Characteristics of the adsorbent

Fig. 1 shows the DFT pore size distributions of the prepared ACFs, CS800 and CS850. Table 1 contains the BET surface area (S_{BET}), t-plot micropore area (S_{micro}), external surface area (including mesopores and macropores area, S_{ext}), total pore volume (V_{total}), t-plot micropore volume (V_{micro}) and average pore width (D_w) results. It is easily found that the two ACFs have remarkable BET surface area, which is predominantly contributed by micropores. The average pore width of CS800 and CS850 is 2.07 nm and 1.72 nm, respectively. Percentage of micropore area is 71.8% and 73.8% respectively, showing that the two adsorbents are dominantly micropores. Fig. 2 shows the FTIR spectra of CS800 and CS850, which display the following bands of 1167 cm^{-1} (C–O), 1563 cm^{-1} (C=O), 2278 cm^{-1} (N=C=O) and 3430 cm^{-1} (N–H) [21,22].

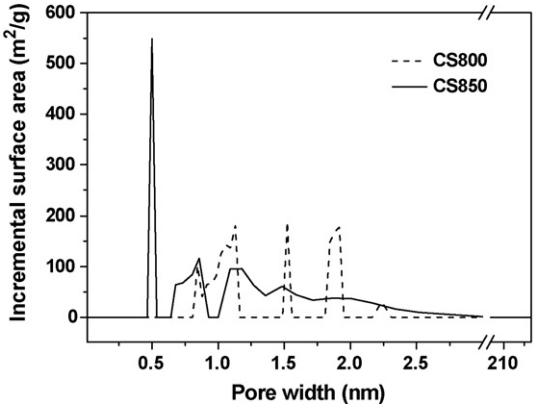

Fig. 1. Pore size distributions of CS800 and CS850 by DFT method.

Table 1
Main characteristic of CS800 and CS850.

Parameter	CS800	CS850
BET surface area (m^2/g)	1376	1736
t-Plot micropore area (m^2/g)	1005	1056
t-Plot external area (m^2/g)	371	680
t-Plot micropore volume (cm^3/g)	0.49	0.46
Total pore volume (cm^3/g)	0.66	0.84
Average pore width (nm)	2.07	1.72
Bulk density (g/cm^3)	0.47	0.43
pH_{pzc}	5.8	6.3
Elemental analysis (wt.%)		
C	87.89	89.12
H	1.41	1.08
N	0.51	0.29
O	10.19	9.51

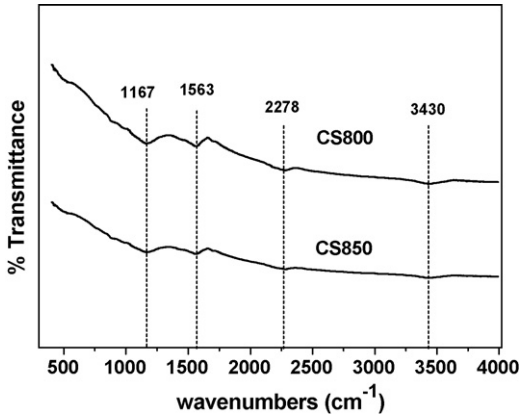

Fig. 2. The FTIR spectra of CS800 and CS850.

3.2. Effect of contact time on the adsorption

Fig. 3 shows the effect of contact time on PNA adsorption on CS800 and CS850. The figure reveals that PNA adsorption on the two adsorbents had similar trends. More than 60% adsorption occurred within 25 min, and the equilibrium was attained within 180 min. The initial higher adsorption rate may be attributed to the large number of most active sites available. The decrease of adsorption rate with contact time could be due to the saturation of active sites and decrease of PNA concentrations [19]. Moreover, the higher PNA adsorption capacity of CS850 than that of CS800 should be due to the difference of pore characteristics of the two adsorbents [23]. As

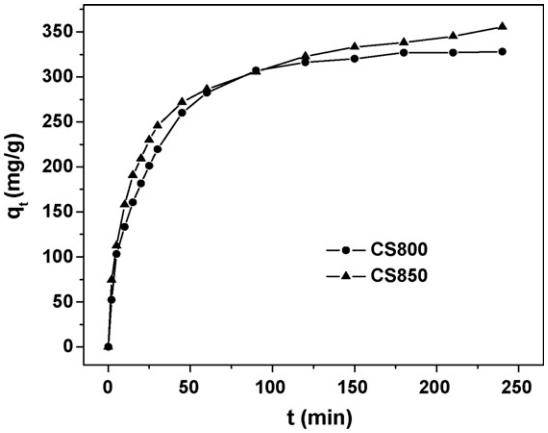

Fig. 3. Effect of contact time on PNA adsorption (V, 500 mL; C_0, 200 mg/L; T, 25 °C; adsorbent dose, 0.2415 g/500 mL; pH, 7.0).

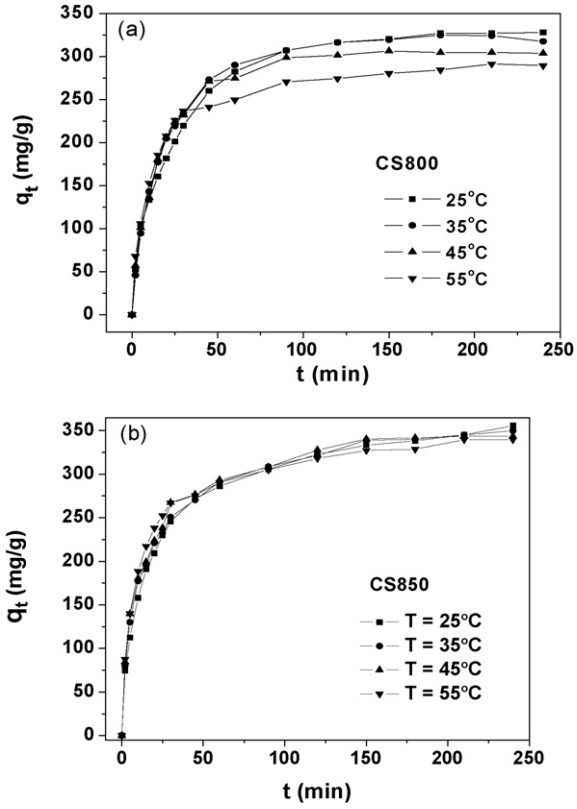

Fig. 4. Effect of solution temperature on the adsorption of PNA on CS800 and CS850 (V, 500 mL; C_0, 200 mg/L; adsorbent dose, 0.2415 g/500 mL; pH, 7.0).

shown in Table 1, the micropore area of CS850 is more than that of CS800, indicating more active sites available on the surface of CS850 than those on CS800 [24]. In addition, the former have higher volume in transition pores (>1.0 nm) for PNA adsorption, which reduces the diffusion path length to primary micropores [25].

3.3. Effect of temperature

Fig. 4a and b shows the effect of solution temperature on PNA adsorption onto CS800 and CS850. It is found that the effect of temperature on the adsorption was related to the contact time and the pore structures of the adsorbents. When solution temperature increased from 25 to 55 °C, the equilibrium adsorption amount of PNA decreased from 328 mg/g to 289 mg/g for CS800 and from 355 mg/g to 339 mg/g for CS850, respectively. The effect of temperature on the PNA adsorption on CS850 was less than that on CS800. It should be due to the higher binding affinity of CS850 with PNA molecules since it has a larger surface area and a smaller pore width than CS800 [26]. The equilibrium PNA adsorption decreased with increasing temperature, indicating that the adsorption was an exothermic process [27].

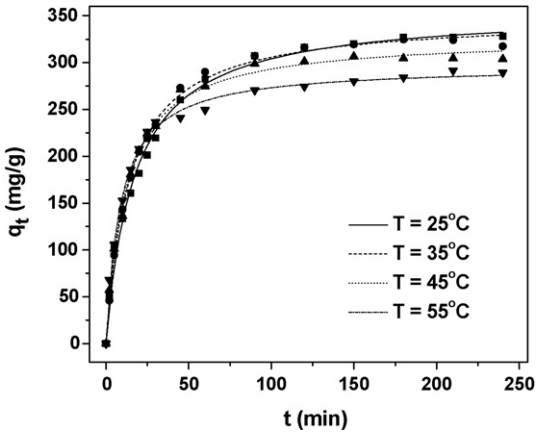

Fig. 5. Ho's pseudo-second-order model kinetic model fit for PNA adsorption on CS850 at different temperatures.

In addition, Fig. 4 reveals that the effect of temperature on PNA adsorption varied with contact time. The adsorption amount q_t at fixed time t changed slightly with temperature as contact time less than 30 min. This phenomenon could be attributed to the heterogeneity of the adsorption sites on the surface of the prepared ACFs. Generally, more active sites are initially occupied by the adsorbates, and then less active sites. Hence, there were many more active sites available on the surface of the prepared ACFs in initial adsorption step. The binding affinity of active sites with the PNA was so high in the beginning 30 min that the effect of temperature on the adsorption could be ignored.

3.4. Adsorption kinetics

In order to investigate the kinetics of adsorption of PNA, the Lagergren-first-order model [28] and Ho's pseudo-second-order model [29] were used.

$$q_t = q_e - q_e e^{-k_1^t} \quad (3)$$

$$q_t = \frac{t}{1/(k_2 q_e^2) + t/q_e} \quad (4)$$

The values of the parameters and the correlation coefficients obtained by using non-linear regression are listed in Table 2. And the Ho's pseudo-second-order kinetic model fit for PNA adsorption on CS850 at four different temperatures is illustrated in Fig. 5. In order to compare the validity of each kinetic model, a normalized

Table 2
Kinetic parameters for PNA adsorption on CS800 and CS850 at different temperatures.

Kinetic model	Parameter	CS800				CS850			
		25 °C	35 °C	45 °C	55 °C	25 °C	35 °C	45 °C	55 °C
Lagergren-first-order	$q_{e,meas}$ (mg/g)	318	315	299	273	326	324	323	314
	k_1 (min^{-1})	0.0440	0.0522	0.0592	0.0773	0.0544	0.0615	0.0668	0.0822
	R^2	0.978	0.989	0.987	0.972	0.958	0.943	0.943	0.950
	Δq (%)	17.54	11.41	13.18	13.14	18.14	18.52	18.06	15.23
	$h_{0,1}$	14	16	18	21	18	20	22	26
Pseudo-second-order	$q_{e,meas}$ (mg/g)	356	348	328	297	360	354	352	340
	k_2 (g/mg min)	0.00016	0.00021	0.00026	0.00039	0.00021	0.00026	0.00029	0.00037
	R^2	0.993	0.998	0.995	0.996	0.991	0.987	0.986	0.992
	Δq (%)	10.54	2.26	5.60	5.30	10.54	9.84	9.51	6.59
	$h_{0,2}$	20	26	28	34	27	33	36	43

standard deviation Δq (%) was calculated using the Eq. (5).

$$\Delta q(\%) = 100\sqrt{\frac{\sum[(q_{t,\exp} - q_{t,\mathrm{cal}})/q_{t,\exp}]^2}{N-1}} \quad (5)$$

From Table 2, it is found that the values of correlation coefficients for the pseudo-second-order model are all higher than those for the Lagergren-first-order model. Moreover, the values of Δq (%) for the Ho's pseudo-second-order model are lower than those for the Lagergren-first-order model. Therefore, the Ho's pseudo-second-order model could be used for the prediction of the kinetics of adsorption of PNA on the adsorbents.

The initial rates of adsorption can be calculated from the Lagergren-first-order and pseudo-second-order model from the following two equations:

$$h_{0,1} = k_1 q_e \quad (6)$$

$$h_{0,2} = k_2 q_e^2 \quad (7)$$

The obtained results are listed in Table 2. It is found that the initial rates of PNA adsorption on CS850 at all different temperatures are higher than those on CS800, which confirms the fact that CS850 exhibits a higher binding affinity with PNA than CS800.

3.5. Mechanism of adsorption

In order to gain insight into the mechanisms and rate-controlling steps affecting the kinetics of adsorption, the kinetic experimental results were fitted to the Morris's intraparticle diffusion [30] and Boyd's film-diffusion model [31]. The rate of intraparticle diffusion is a function of $t^{0.5}$ and can be defined as follows:

$$q_t = f\left(\frac{D_t}{r_p^2}\right)^{0.5} = K_w t^{0.5} + c_w \quad (8)$$

The K_w values can be obtained by plotting q_t against time. The intercept value, c_w, represents the resistance to mass transfer in the external liquid film. If the plot is linear and passes through the origin then pore diffusion controls the rate of mass transfer. If the plot is non-linear or linear but does not pass through the origin, then it is concluded that film-diffusion or chemical reaction control the adsorption rate. The previous studies [15,32] showed that the plot usually presents multi-linearity, indicating that the overall adsorption process may be controlled by more steps such as film diffusion, intraparticle diffusion and a chemical reaction on the pore surface.

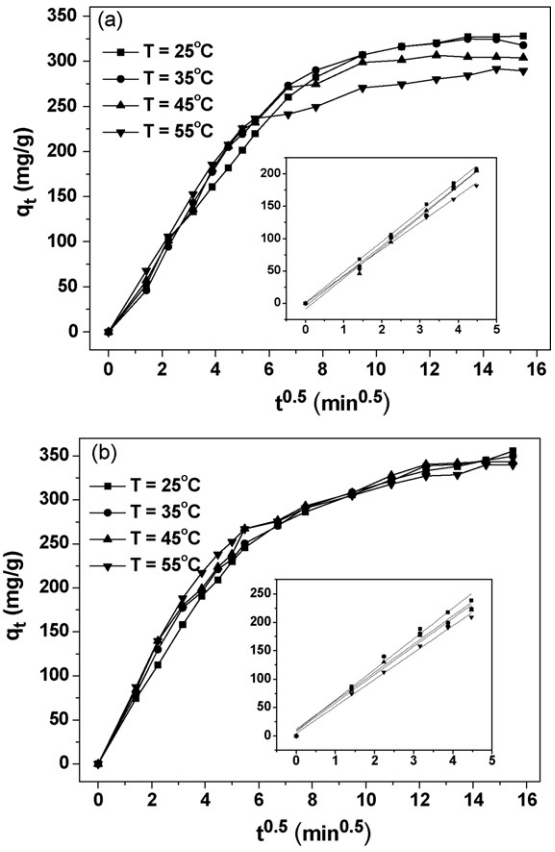

Fig. 6. Intraparticle diffusion plots for PNA adsorption on CS800 (a) and CS850 (b) at different temperatures.

As shown in Fig. 6a and b, the plots for intraparticle diffusion model for the two adsorbents at four different temperatures are not straight lines, indicating the film-diffusion mechanism is the rate-controlling step in the whole adsorption process. However, the regression was linear and passed nearly through the origin in the first 20 min. The result suggested that the pore diffusion played an important role in this stage. The values of K_w and intercept c_w evaluated from the first linear parts for the two prepared ACFs at four different temperatures are shown in Table 3. The K_w values for CS850 are all higher than those for CS800 at four different temperatures, implying the initial rates of PNA adsorption on CS850

Table 3
Diffusion coefficients for PNA adsorption on CS800 and CS850 at different temperatures.

Model	Carbon	T (°C)	Intercept c_w	K_w (mg/g $min^{0.5}$)	R^2
Morris's intraparticle diffusion	CS800	25	0.775	41.339	0.991
		35	−7.797	46.377	0.990
		45	−4.114	46.519	0.995
		55	1.104	47.071	0.999
	CS850	25	4.555	47.344	0.996
		35	8.718	48.586	0.984
		45	11.845	49.900	0.976
		55	9.266	53.844	0.987
		T (°C)	Intercept c_b	B	R^2
Boyd's film-diffusion	CS800	25	−0.005	0.020	0.997
		35	−0.032	0.028	0.986
		45	−0.037	0.033	0.974
		55	−0.028	0.039	0.994
	CS850	25	−0.004	0.023	0.997
		35	0.007	0.027	0.992
		45	0.015	0.029	0.990
		55	0.002	0.037	0.999

Table 4
Isotherm parameters for PNA adsorption on CS800 and CS850 at 25 °C.

Adsorbent	Langmuir model				Freundlich model			
	q^0	K_L	R^2	Δq (%)	K_F	n_F	R^2	Δq (%)
CS800	420.97	0.1848	0.841	13.68	150.3	4.56	0.999	0.97
CS850	510.98	0.1284	0.924	18.53	144.7	3.72	0.989	8.65

were higher than those on CS800 [30]. The values of intercept c_w for CS850 are all higher than that for CS800, indicating the more resistance to mass transfer in the external liquid film for CS850 than that for CS800 [32].

The Boyd's film-diffusion model is expressed as:

$$F = 1 - \left(\frac{6}{\pi^2}\right)\sum_{n=1}^{\infty}\left(\frac{1}{n_b^2}\right)\exp(-n_b^2 Bt) \quad (9)$$

The value of F can be obtained by the expression:

$$F = \frac{q_t}{q_e} \quad (10)$$

Rearranging the above equations gives:

$$F \text{ values} > 0.85 \quad Bt = -0.4977 - \ln(1-F) \quad (11)$$

and for

$$F \text{ values} < 0.85 \quad Bt = \left(\sqrt{\pi} - \sqrt{\pi - \frac{\pi^2 F}{3}}\right)^2 \quad (12)$$

The values of Bt can be calculated from Eqs. (10)–(12). B can be used to calculate the effective diffusion coefficient, D_i (cm^2/s), from the equation:

$$B = \frac{\pi^2 D_i}{r_p^2} \quad (13)$$

Eqs. (10)–(12) can be used in predicting the mechanism of the adsorption process. This is done by plotting Bt against time t. B and c_b are the slope and intercept of the line, respectively. If the plot is linear and passes through the origin, then pore diffusion controls the rate of mass transfer. If the plot is non-linear or linear but does not pass through the origin, then it is concluded that film-diffusion or chemical reaction control the adsorption rate [31].

The Bt values were plotted against time t in 20 min for the two adsorbents at four different temperatures. The values of B and c_b are shown in Table 3. It is found that the values of intercept c_b are all nearly zero, further confirming that the adsorption was mainly controlled by pore diffusion in the first adsorption step [33].

3.6. Adsorption equilibrium

The adsorption isotherms measured for PNA on CS800 and CS850 at 25 °C are plotted in Fig. 7. Both the isotherms belong to the L-type of the classification proposed by Giles et al. [34]. Such type of isotherms may be fitted to the Langmuir [35] and Freundlich [36] models:

$$q_e = \frac{K_L q^0 C_e}{1 + K_L C_e} \quad (14)$$

$$q_e = K_F C_e^{1/n} \quad (15)$$

The equilibrium adsorption studies were conducted using various adsorbent dose of 0.10–1.30 g/L at pH 7.0 at 25 °C. Isotherm parameters of the two models obtained by using non-linear regression are listed in Table 4. It is found that the fitting to the Freundlich equation gave the higher values of correlation coefficients than those for the Langmuir equation. Further more, the values of Δq (%) for the Freundlich equation are all lower than those for the

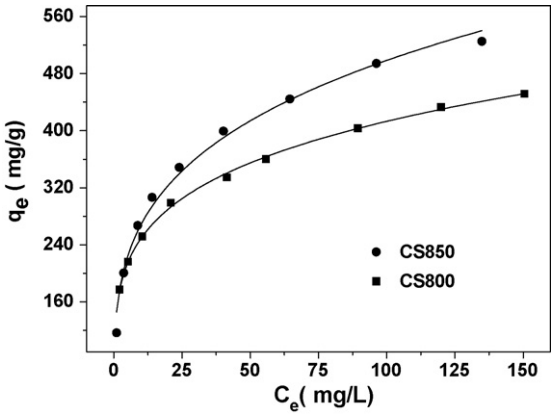

Fig. 7. Isotherm plots for PNA on CS800 and CS850 at 25 °C (V, 100 mL; C_0, 200 mg/L; T, 25 °C; adsorbent dose, 0.10–1.30 g/L; pH, 7.0).

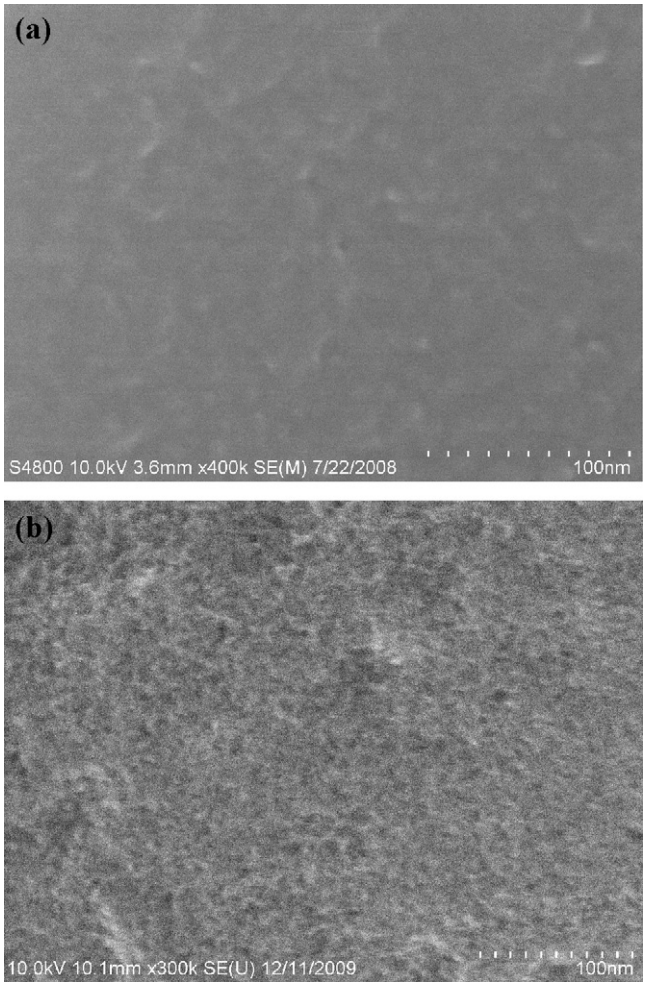

Fig. 8. The SEM photographs of CS850 (a) before PNA adsorption and (b) after PNA adsorption.

Langmuir equation. The above results showed that the empirical Freundlich equation was better than the Langmuir equation in describing the behavior of PNA adsorption onto the two adsorbents, implying that the adsorption process involved multimolecular layers of coverage [37].

SEM is widely used to study the morphological features and surface characteristics of the adsorbent materials [37,38]. In the present study, SEM is used to assess morphological changes in the carbon surfaces following adsorption of the PNA molecules. The SEM photographs of CS850 before and after PNA adsorption are shown in Fig. 8. It is found that the surface micrograph of CS850 after PNA adsorption showed a distinct roughness with oval patterns as shown in Fig. 7b. The observed phenomenon also provided further evidence that the adsorption process involved multimolecular layers of coverage on CS850 surface. The previous studies [38,39] also showed that the external surface displayed more curved planes and holes after adsorption. This phenomenon was ascribed to heterogeneous energy distribution of the activated adsorption sites on the surface of the activated carbons [39].

4. Conclusion

The present study shows that the ACFs prepared from cotton stalk fiber can be used as adsorbents for the removal of PNA from aqueous solutions. The prepared cotton stalk ACFs have very large BET surface area, which is primarily almost contributed by micropores. The maximum PNA adsorption on the ACFs was found to be more than 510 mg/L, and over 60% adsorption occurred in the beginning 25 min. The pseudo-second-order equation was found to explain the adsorption kinetics most effectively. The equilibrium adsorption amount increased with the increase of micropore area. The pore diffusion played an important role in the PNA adsorption on the prepared ACFs, and intraparticle diffusion was the rate-limiting step in the beginning 20 min. The equilibrium adsorption amount decreased with increasing temperature, indicating that the adsorption is an exothermic process. The Langmuir and Freundlich models were used to interpret the adsorption phenomenon of the adsorbate, and the results implied that the surface of the cotton stalk activated carbons is heterogeneous, which is consistent with the observed phenomenon of SEM.

Acknowledgements

The authors thank the Nanjing Agricultural University Youth Science & Technology Innovation Foundation and the National Water Spectial Project of China (No. 2008ZX07101-005) for financial support.

References

[1] F. Bhunia, N.C. Saha, A. Kaviraj, Effects of aniline-an aromatic amine to some freshwater organisms, Ecotoxicology 12 (2003) 397–403.
[2] K.T. Chung, S.C. Chen, Y.Y. Zhu, Toxic effects of some benzamines on the growth of azotobacter vinelandii and other bacteria, Environ. Toxicol. Chem. 16 (1997) 1366–1369.
[3] D.H. Blakey, K.L. Maus, R. Bell, et al., Mutagenic activity of industrial chemicals in a battery of in vitro and in vivo tests, Mut. Res. 320 (1994) 273–283.
[4] N.I. Sax, Dangerous Properties of Industrial Materials, Van Nortrand Reinhold Company Inc., New York, 1984.
[5] D.S. Lee, K.S. Park, Y.W. Nam, et al., Hydrothermal decomposition and oxidation of *p*-nitroaniline in supercritical water, J. Hazard. Mater. 56 (1997) 247–256.
[6] J.H. Sun, S.P. Sun, M.H. Fan, A kinetic study on the degradation of *p*-nitroaniline by Fenton oxidation process, J. Hazard. Mater. 148 (2007) 172–177.
[7] S. Gautam, S.P. Kamble, S.B. Sawant, et al., Photocatalytic degradation of 4-nitroaniline using solar and artificial UV radiation, Chem. Eng. J. 110 (2005) 129–137.
[8] A. Saupe, High-rate biodegradation of 3- and 4-nitroaniline, Chemosphere 39 (1999) 2325–2346.
[9] K. Zheng, B.C. Pan, Q.J. Zhang, Enhanced adsorption of *p*-nitroaniline from water by a carboxylated polymeric adsorbent, Sep. Purif. Technol. 57 (2007) 250–256.
[10] Y.Q. Wu, M. Zhou, M.G. Ma, et al., Adsorption kinetics of *p*-nitroaniline on the insolubilized humic acid, Technol. Water Treat. (Chin.) 33 (2007) 14–17.
[11] M.G. Ma, Y.X. Wei, Y. Zhang, et al., Modify of clinoptilolit (from Baiyin) and its adsorption of *p*-nitroaniline, J. Anhui Agri. Sci. (Chin.) 35 (2007) 2061–2062.
[12] L.R. Shen, P.Z. Yang, L.Y. Chen, Treatment of waster water containing *p*-nitroaniline with emulsion liquid membrane process, Technol. Water Treat. (Chin.) 23 (1997) 45–49.
[13] M.A. Oturan, J. Peiroten, P. Chartrin, et al., Complete destruction of *p*-nitrophenol in aqueous medium by electro-Fenton method, Environ. Sci. Technol. 34 (2000) 3474–3479.
[14] M. Suzuki, Activated carbon fiber: fundamentals and applications, Carbon 32 (1994) 577–586.
[15] C. Brasquet, P. Le Cloriec, Adsorption onto activated carbon fibers: application to water and air treatments, Carbon 35 (1997) 1307–1313.
[16] I. Martin-Gulloan, R. Font, Dynamic pesticide removal with activated carbon fibers, Water Res. 35 (2001) 516–520.
[17] P.A. Quinlivan, L. Li, D.R.U. Knappe, Effects of activated carbon characteristics on the simultaneous adsorption of aqueous organic micropollutants and natural organic matter, Water Res. 39 (2005) 1663–1673.
[18] K.Q. Li, Z. Zheng, X.F. Huang, et al., Adsorption of *p*-nitroaniline from aqueous solution onto activated carbon fiber prepared from cotton stalk, J. Hazard. Mater. 166 (2009) 1180–1185.
[19] Z.B. Sun, L.J. Ma, Discussed and industrialization utilization of the cotton stalk, Building Artif. Boards (Chin.) 3 (2001) 20–24.
[20] B.M. Babic, S.K. Milonjic, M.J. Polovina, et al., Point of zero charge and intrinsic equilibrium constants of activated carbon cloth, Carbon 37 (1999) 477–481.
[21] Y.X. Zhao, X.Y. Sun, The Spectrographical Identification of Organic Molecular Structure, Science Press, Beijing, 2003.
[22] S.G. Reznik, I. Katz, C.G. Dosoretz, Removal of dissolved organic matter by granular-activated carbon adsorption as a pretreatment to reverse osmosis of membrane bioreactor effluents, Water Res. 42 (2008) 1595–1605.
[23] J.F. Langford, M.R. Schure, Y. Yao, et al., Effects of pore structure and molecular size on diffusion in chromatographic adsorbents, J. Chromatogr. A 1126 (2006) 95–106.
[24] A. Teresa, G.M. Centeno, B. Antonio, Importance of micropore size distribution on adsorption at low adsorbate concentrations, Carbon 41 (2003) 841–846.
[25] Y. Guo, S. Kaplan, T. Karanfil, The significance of physical factors on the adsorption of polyaromatic compounds by activated carbons, Carbon 46 (2008) 1885–1891.
[26] A. Ornek, M. Ozacar, I.A.S. Engil, Adsorption of lead onto formaldehyde or sulphuric acid treated acorn waste: equilibrium and kinetic studies, Biochem. Eng. J. 37 (2007) 192–200.
[27] M. Karaa, H. Yuzera, E. Sabah, Adsorption of cobalt from aqueous solutions onto sepiolite, Water Res. 37 (2003) 224–232.
[28] S. Lagergren, About the theory of so-called adsorption of soluble substances, Kungliga Svenska Vetenskapsakademiens Handlingar 24 (1898) 1–39.
[29] Y.S. Ho, Adsorption of heavy metals from waste streams by peat, Ph.D. Thesis, University of Birmingham, Birmingham, UK, 1995.
[30] W.J. Weber, J.C. Morris, Kinetics of adsorption on carbon from solution, J. Sanitary Eng. Div. Proceed. Am. Soc. Civil Eng. 89 (1963) 31–59.
[31] G.E. Boyd, A.W. Adamson, L.S. Myers, The exchange adsorption of ions from aqueous solutions by organic zeolites, II: kinetics, J. Am. Chem. Soc. 69 (1947) 2836–2848.
[32] P. Le Cloirec, C. Brasquet, E. Subrebat, Adsorption onto fibrous activated carbon: applications to water treatment, Energy Fuels 11 (1997) 331–336.
[33] B.H. Hameed, M.I. El-Khaiary, Equilibrium, kinetics and mechanism of malachite green adsorption on activated carbon prepared from bamboo by K_2CO_3 activation and subsequent gasification with CO_2, J. Hazard. Mater. 157 (2008) 344–351.
[34] C.H. Giles, D. Smith, A. Huitson, General treatment and classification of the solute adsorption isotherm. I. Theoretical, J. Colloid Interface Sci. 47 (1974) 755–765.
[35] I. Langmuir, The adsorption of gases on plane surfaces of glass, mica and platinum, J. Am. Chem. Soc. 40 (1918) 1361–1403.
[36] H.M.F. Freundlich, Over the adsorption in solution, J. Phys. Chem. 57 (1906) 385–471.
[37] S. Gupta, A. Pal, P.K. Ghosh, et al., Performance of waste activated carbon as a low-cost adsorbent for the removal of anionic surfactant from aquatic environment, J. Environ. Sci. Health A 38 (2003) 381–397.
[38] B. Tansel, P. Nagarajan, SEM study of phenolphthalein adsorption on granular activated carbon, Adv. Environ. Res. 8 (2004) 411–415.
[39] D.Y. Tang, Z. Zheng, K. Lin, et al., Adsorption of *p*-nitrophenol from aqueous solutions onto activated carbon fiber, J. Hazard. Mater. 143 (2007) 49–56.